

SUPPORTING INFORMATION

Structural control of $^1A_{2u}$ to $^3A_{2u}$ intersystem crossing in diplatinum (II,II) complexes

Alec C. Durrell;^a Gretchen E. Keller;^a Yan-Choi Lam;^a Jan Sýkora;^a Antonín Vlček, Jr.;^{*,b,c} and
Harry B. Gray^{*,a}

^a Beckman Institute, California Institute of Technology, Pasadena, CA 91125, USA

^b J. Heyrovský Institute of Physical Chemistry, Academy of Sciences of the Czech Republic,
Dolejškova 3, CZ-182 23 Prague, Czech Republic

^c Queen Mary University of London, School of Biological and Chemical Sciences, Mile End
Road, London E1 4NS, United Kingdom
e-mail: a.vlcek@qmul.ac.uk; hgray@caltech.edu

Per(difluoroboro)tetrakis(pyrophosphito)diplatinatate(II), $[n\text{-Bu}_4\text{N}]_4[\text{Pt}_2(\mu\text{-P}_2\text{O}_5(\text{BF}_2)_2)_4]$: Under a dry argon atmosphere, 400 mg $[n\text{-Bu}_4\text{N}]_4[\text{Pt}_2(\mu\text{-P}_2\text{O}_5\text{H}_2)_4]$ (0.21 mmol) were dissolved in 3 mL of neat $\text{F}_3\text{B}\cdot\text{OEt}_2$ and stirred at room temperature for two days. The solvent was removed by vacuum distillation, and the solid was washed with dry, degassed THF. The residue was dissolved in acetonitrile and the solution was filtered through Celite. The product precipitated after addition of THF. The luminescent green powder was washed with more THF to yield 350 mg product (0.15 mmol, yield 73%). Further purification was achieved by vapor diffusion of diethyl ether into an acetonitrile solution of the product. Photophysical measurements were made on samples that had been recrystallized two times. Characterization: ^1H NMR (300 MHz, CD_3CN) δ 3.08-3.14 (m, 2 H), 1.57-1.69 (m, 2 H), 1.39 (quintet, $J = 8$ Hz, 2 H), 1.00 (t, $J = 8$ Hz, 3 H); ^{19}F NMR (282 MHz, CD_3CN) δ -133.54, (d, $J = 62$ Hz), -138.78 (d, $J = 62$ Hz); ^{31}P NMR (121 MHz, CD_3CN) δ 58.81 ($J_{\text{P-Pt}} = 3112$ Hz).

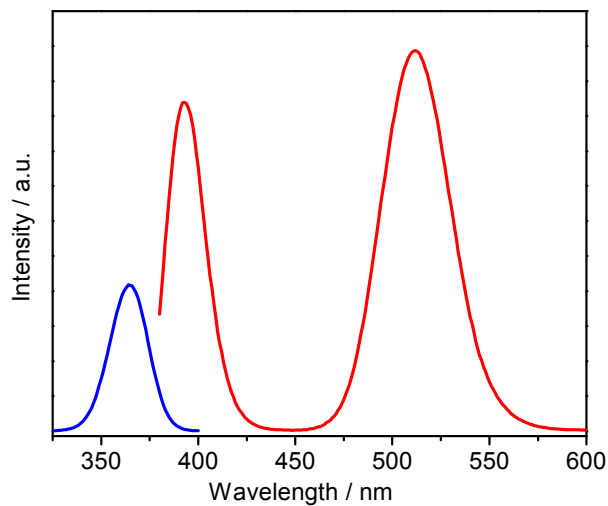


Figure S1. Red: emission spectrum of Pt(pop-BF₂) measured using 373 nm excitation. Blue: normalized excitation spectra of in MeCN obtained at $\lambda_{em} = 405$ and 512 nm. The two spectra are indistinguishable after normalization of the peak intensities. Measured in a MeCN solution at 21 °C, freeze-pump-thaw degassed at 4×10^{-5} mbar.

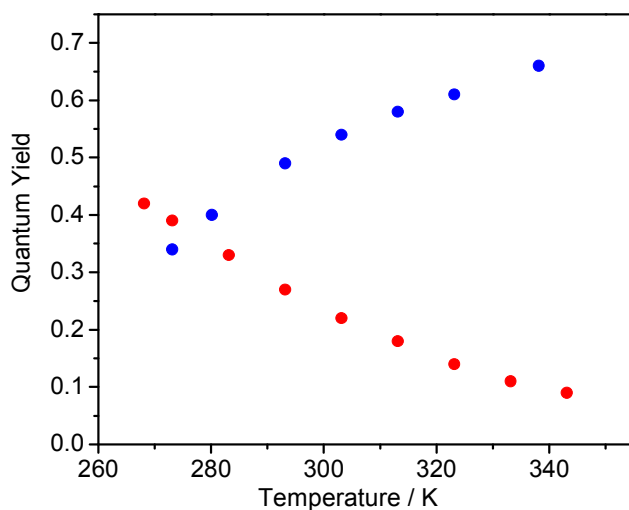


Figure S2. Temperature-dependence of the fluorescence (red) and phosphorescence (blue) quantum yield of Pt(pop-BF₂) in MeCN.

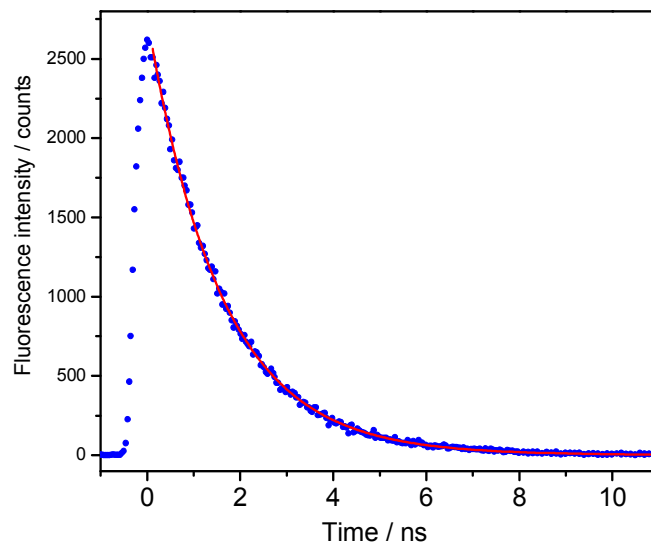


Figure S3. Fluorescence decay of Pt(pop-BF₂) in MeCN measured with a streak camera, excited at 355 nm, 50 ps pulse. Emission in the 400-415 nm range was selected by a bandpass filter. Red curve: single-exponential fit with $\tau = 1.58 \pm 0.01$ ns.

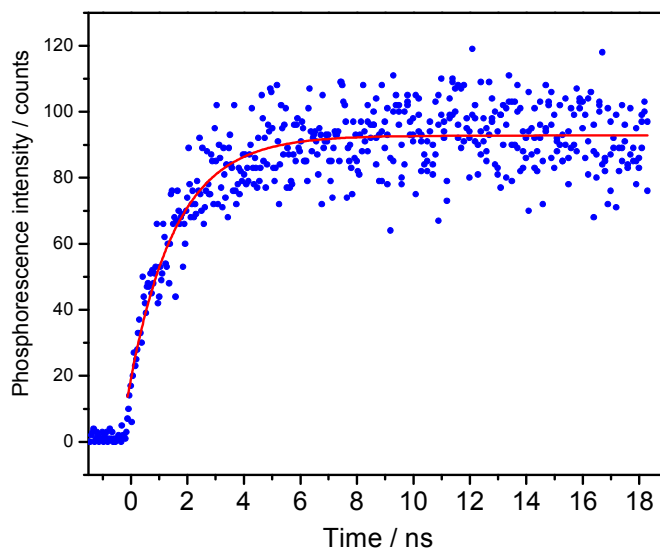


Figure S4. Phosphorescence rise of Pt(pop-BF₂) in MeCN measured with a streak camera, excited at 355 nm, 50 ps pulse. Emission wavelengths >500 nm were selected by a cut-off filter. Red curve: single-exponential fit with $\tau = 1.62 \pm 0.09$ ns.

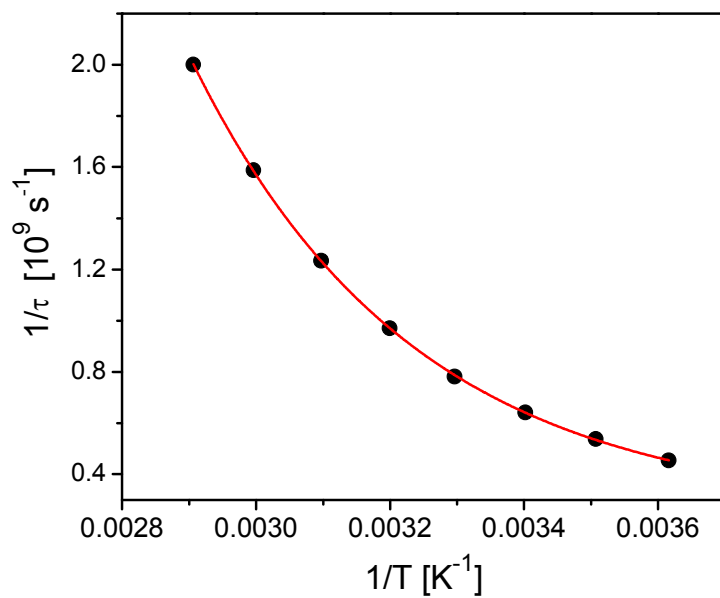


Figure S5. Temperature dependence of Pt(pop-BF₂) fluorescence lifetime fitted to equation 6.

Table S1. The temperature dependence of Pt(pop-BF₂) fluorescence (ϕ_f) and phosphorescence (ϕ_{ph}) quantum yields. Measured in degassed MeCN solution.

T [°C]	T [K]	ϕ_f	ϕ_{ph}	$\phi_f + \phi_{ph}$
-5	268.15	0.42	-	-
0	273.15	0.39	0.34	0.73
7	280.15	-	0.40	-
10	283.15	0.33	-	-
20	293.15	0.27	0.49	0.76
30	303.15	0.22	0.54	0.76
40	313.15	0.18	0.58	0.76
50	323.15	0.14	0.61	0.75
60	333.15	0.11	-	-
65	338.15	-	0.66	-
70	343.15	0.09	-	-

Table S2. Temperature dependence of Pt(pop-BF₂) fluorescence lifetime. The values were obtained by deconvolution of the TCSPC signal and the actual excitation pulse profile. The nonradiative ¹A_{2u} decay rate constants k_{nr} were calculated as $1/\tau - k_r$; assuming $k_r = 1.7 \times 10^8 \text{ s}^{-1}$, as estimated from the fluorescence quantum yield and lifetime at 20 °C

t [°C]	T [K]	τ_1 [ns]	τ_2 [ns]	A ₁ [%]	A ₂ [%]	k_{nr} [10^8 s^{-1}]
3.4	276.55	0.29	2.20	5	95	2.8
12.0	285.15	0.12	1.86	8	95	3.7
20.8	293.95	0.20	1.56	9	91	4.7
30.2	303.35	0.20	1.28	9	91	6.1
39.4	312.55	0.14	1.03	10	90	8.0
49.7	322.85	0.12	0.81	11	89	10.6
60.6	333.75	0.08	0.63	12	88	14.2
70.9	344.05	0.06	0.50	13	87	18.3